Solidified Salt Melts of the NaCl–KCl–CeF_3–EuF_3 System as Promising Luminescent Materials

Viktor Zinchenko , Ganna Volchak * , Nataliia Chivireva , Pavlo Doga , Yaroslav Bobytskyy , Oleh Ieriomin , Serhii Smola , Anton Babenko , Małgorzata Sznajder

Posted Date: 17 October 2024

doi: 10.20944/preprints202410.1383.v1

Keywords: Cerium fluoride; Europium fluoride; NaCl–KCl melt; solidified solution-melt; oxidation-reduction; photoluminescence

Article

Solidified Salt Melts of the NaCl–KCl–CeF_3–EuF_3 System as Promising Luminescent Materials

Viktor Zinchenko [1], Ganna Volchak [1,*], Nataliia Chivireva [1], Pavlo Doga [1], Yaroslav Bobitskyy [2], Oleh Ieriomin [1], Serhiy Smola [1], Anton Babenko [1] and Małgorzata Sznajder [2]

[1] O. Bogatsky Physico-Chemical Institute NASU, Lustdorfska doroga 86, Odesa 65080, Ukraine
[2] Institute of Physics University of Rzeszow, Pigonia 1, Rzeszow 35-310, Poland
* Correspondence: volchakganna@gmail.com

Abstract: The results of the study of the interaction between the CeF_3+EuF_3 system and the salt melt NaCl–KCl by spectroscopic methods are presented. It was established that no significant changes occur with CeF_3 ions upon dissolution in the NaCl–KCl melt. Instead, the transition of EuF_3 into solution-melt, both individually and in the CeF_3+EuF_3 system, is accompanied by oxidation-reduction reactions with the formation of Eu^{2+}. Diffuse reflection spectra of the samples – both bottom (insoluble sediment) and upper parts of the solidified salt melt in the UV range indirectly indicate the excitation of photoluminescence of Ce^{3+} and Eu^{2+} ions. On the other hand, the presence of absorption bands in the near-IR range of the spectrum (1900-2300 cm^{-1}) confirms the preservation of a certain proportion of Eu^{3+} ions in the salt melt. The influence of various factors (composition of the solidified salt melt sample, excitation wavelength, previous and subsequent heat treatment, and composition of the medium) on the nature of the excitation and emission spectra of the samples was studied. A very intense 5d-4f luminescence of Ce^{3+} and Eu^{2+} ions (at 330 and 430 nm, respectively), mainly in the upper part of salt melts, and much weaker 4f-4f luminescence of Eu^{3+} ions were observed. Certain parameters were optimized to reduce the proportion of luminescence of Ce^{3+} and, especially, Eu^{3+} ions and to increase the luminescence of Eu^{2+} ions. Solidified salt solutions-melts of the NaCl–KCl–CeF_3–EuF_3 system are promising materials for the creation of solar ultraviolet radiation detectors.

Keywords: Cerium fluoride; Europium fluoride; NaCl–KCl melt; solidified solution-melt; oxidation-reduction; photoluminescence

1. Introduction

The sun is a source of various radiation: visible light, thermal (infrared), ultraviolet, X-ray radiation, etc. Thanks to the Earth's atmosphere, a significant part of hard, in particular, ultraviolet radiation does not reach the surface. The part that reaches the lower layers of the atmosphere is classified into three bands: UVA (315-400 nm), UVB (280-315 nm) and UVC (200-280 nm). The ozone layer largely attenuates the low-energy side of the UVC and UVB bands, and this causes strong fluctuations in radiation intensity in the range between 250 and 410 nm.

Sunlight reaching the Earth's surface has a certain spectral intensity dependence, as shown in [1]. In the range of 315÷375 nm, the intensity of the Sun's ultraviolet radiation is almost independent of the wavelength. To measure the intensity (flow) of ultraviolet radiation, the use of thermo-luminescence methods is promising, since its integrated area is related to the concentration of the accumulated charge in the dosimeter material [2]. The review [3] analyzed the latest developments of ultraviolet radiation detectors. Among them, one should mention detectors of photoconductive type, Schottky barrier type, metal-semiconductor-metal type, as well as several developments of modern types based on nanostructured materials.

Cerium and europium belong to lanthanides of variable valence, since, in addition to the +3 oxidation state usual for chemists, in their compounds, in particular, fluorides, under certain conditions, they also show +4 and +2 oxidation states, respectively.

 doi:10.20944/preprints202410.1383.v1

In general, Eu^{2+} and Ce^{3+} ions are more stable in a reducing atmosphere, while the stability of Eu^{3+} and Ce^{4+} is promoted by an oxidizing environment. The luminescent properties of Eu^{2+} and Ce^{3+} are determined by the 5d-4f electronic transitions, and therefore strongly depend on the influence of the surrounding environment, for example, symmetry, coordination number, crystal field strength, etc. This is due to the fact that the excited 5d state is not shielded by 5s2 and 5p6 electrons [4,5]. In turn, Eu^{3+} ions enable orange-red luminescence due to 4f-4f electronic transitions, namely, $^5D_0 \rightarrow {}^7F_2$ at a wavelength of 617 nm, which has been used for quite a long time in industrial red phosphors Y_2O_3:Eu^{3+} and Y_2O_2S:Eu^{3+}. The authors [6,7] established the possibility of coexistence of different-valent forms of Europium (II, III) and Cerium (III, IV) in one matrix and the possibility of energy transfer between different forms.

It was found in paper [8] that halides doped with Europium show thermo-luminescence signals when they are excited by radiation with a wavelength of 220-280 nm. This phenomenon has been applied to detect solar UVC radiation from KCl:Eu^{2+} single crystals as thermo-luminescent dosimeters. The effectiveness of the KCl:Eu^{2+} system as a selective UVC dosimeter is described in Refs. [9,10]. The TL excitation spectrum of KCl:Eu^{2+} single crystals was measured and its convolution with the solar spectral radiation reaching the Earth was estimated according to the radiation transfer model. By comparing the thermo-luminescence sensitivity of the ultraviolet dose of KCl:Eu^{2+} with the measured dose of solar radiation, the authors concluded that, although UVC radiation at the ground level is six orders of magnitude less than UVB, it is nevertheless detectable and can be measured using KCl:Eu^{2+} dosimeters.

In turn, the authors of [11] simulated the flow of solar ultraviolet radiation, which was registered by a dosimeter during the day. The authors confirm the fact that the Eu^{2+}-doped KCl crystal behaves under the sunlight as a narrow-band Gaussian detector centred on a wavelength of 265 nm. On the other hand, a comparison of the KCl:Eu^{2+} system and commercially available broad-band UVB biological sensors (biometers) shows that Europium-doped crystals are more sensitive to small changes in solar UVB flux, so they are a good choice for detecting significant ozone depletion.

The study of optical phenomena in KCl single crystals doped with Ce^{3+} was carried out in [12]. The observed blue glow is caused by the emission of Ce^{3+} ions, which indicates the participation of the latter in the thermo-luminescence process. The authors note the low content of Ce^{3+} ions in the KCl matrix which reduces the efficiency of the process. The article [13] presents the results of the study of the optical characteristics of KCl single crystals co-doped with Eu^{2+} and Ce^{3+}. It is noted that crystals doped together show an increased intensity of thermo-luminescence compared to samples doped with one of the ions. These results confirm the phenomenon of energy transfer between Ce^{3+} and Eu^{2+} in the KCl matrix and the perspective of using the material to create a thermally stimulated dosimeter.

However, the need to use as a matrix KCl single crystals, grown in a laborious way, with the embedding of very hygroscopic compounds ($EuCl_2$, $CeCl_3$) in the matrix, which are easily hydrolyzed and oxidized in air, become an obstacle to the wider use of such materials. Therefore, some authors turned their attention to eutectic materials as matrices for luminescent dosimeters. Thus, the authors [14] proposed the use of self-organized eutectics and systems based on them as scintillation materials for ionizing radiation detectors.

Interesting results of the study of halide melts containing Europium are presented in [15]. It was established there that both ionic and electronic conductivity is observed in the NaCl–KCl melt containing Eu(II) and Eu(III) complexes. In turn, the authors of [16] measured the electronic absorption spectra of Nd^{3+} introduced into LiCl–KCl and NaCl–CsCl eutectics.

Considering the variety of UV radiation detectors and promising materials for these detectors, it can be concluded that it is very important to systematically measure the UV radiation flux reaching the surface of our planet, sine that a potentially sharp increase in the UV radiation flux reaching the surface can be expected. Therefore, there is a need for the development of durable and reliable sensors for monitoring incoming solar ultraviolet radiation. One of the promising methods of synthesis of materials for detection is self-organizing eutectics and systems based on eutectics, in particular, NaCl–KCl.

 doi:10.20944/preprints202410.1383.v1

We have previously [17] investigated the solubility of lanthanide fluorides (La÷Lu) in a salt melt of NaCl–KCl of equimolar composition and the possibility of its detection by the methods of diffuse reflectance spectroscopy and luminescence of solidified melts. For the first time, the course of redox reactions between EuF_3 and the components of the salt melt with the transformation of Eu(III) into Eu(II) was revealed, which was evidenced by the almost complete disappearance of the absorption band characteristic of EuF^3 in the range of 1900-2200 nm and the manifestation of luminescence in the range characteristic of Eu^{2+} at 425-430 nm [18]. A similar phenomenon was found in the solidified melt of NaCl–KCl with CeF_3+EuF_3 [19].

The main goal of the present paper is a detailed study of the effect of CeF_3 on the luminescence characteristics of Eu^{2+} and Eu^{3+} ions in the NaCl–KCl melt. The next purpose of the work is to optimize the ratio between CeF_3, EuF_3 as well as the CeF_3+EuF_3 mixture and NaCl–KCl solidified salt melt. Additionally, we aim to optimize the heat treatment method in order to increase the emission efficiency of Eu^{2+} ions in the salt melt.

2. Materials and Methods

2.1. Manufacturing of Cerium and Europium Fluorides and the NaCl–KCl Salt System

The synthesis of samples of the CeF_3–EuF_3 system with molar ratios of 1:1, 2:1 and 1:2 between CeF_3 and EuF_3 and mass ratios of 1:9 (in the first case) and 2:8 (in the second case) between fluoride systems and the NaCl–KCl salt system was carried out by melt method. For this, carefully ground powders of previously synthesized fluorides in a certain molar ratio were mixed, pressed into tablets and placed in tubes made of quartz glass, which were evacuated, and in turn, placed in reactors that were filled with Helium and sealed. High-purity lanthanide oxides served as starting preparations. Cerium (III) fluoride (CeF_3) was obtained from Cerium dioxide (CeO_2) of the CeO-D grade (OST 48-195-81) by the treatment with ammonium fluoride with the addition of H_2O_2 as a reducing agent, followed by re-melting in a graphite crucible. Europe (III) fluoride (EuF_3) was obtained by treating Europium (III) oxide of the EiO-Zh grade (OST 48-199-81) with concentrated H_2F_2 of special purity followed by vacuum drying and high-temperature calcination in an inert gas medium (He).

Samples of the CeF_3+EuF_3 system were calcined in an inert medium (He) at 1100°C for 4 hours in a vertical furnace, after which they were removed and cooled in air. After cooling, the samples of the system were ground and mixed with the solution of the salt system NaCl–KCl of equimolar composition in the mass ratio of fluoride: salt mixture as 1:9 and 2:8. The mixtures were again placed in a quartz glass tubes with a height of 10 cm and a diameter of about 1 cm, which, in turn, were placed in a quartz glass reactor, evacuated and filled with inert gas (He) and then placed into a vertical furnace.

Heat treatment of samples in molten NaCl–KCl was carried out at a temperature of 750-800°C (that is, 80-130°C higher than the melting point of NaCl–KCl), at which the salt part is in a molten state and is saturated with fluoride within 2-4 hours. Then the oven was turned off, and after complete cooling, the tubes were removed from it. In solidified salt melt, in most cases, the dividing line between the bottom part (that is, insoluble sediment) and the upper part (that is, solidified solution-melt) is clearly visible due to a significant difference in the density and refractive indices of substances. In the case of the NaCl–KCl–CeF_3–EuF_3 (2:1) sample, the intermediate (middle) part of the solidified salt melt was also taken for study. Samples of solidified salt melts are colorless with a weak barely noticeable luminescence under direct sunlight.

2.2. X-ray Diffraction Method

X-ray diffraction method (XRD) of the products was performed on a DRON-3M diffractometer with CuKα radiation (0.15418 nm) using the powder method. XRD images were taken with focusing according to the Bragg-Brentano scheme in the range of angles 10-80° with a step of 0.5° and an exposure of 1 s. The dimensions of the Soler slits were 002/12/025 mm. The error of the device was 0.01%.

 doi:10.20944/preprints202410.1383.v1

To identify the phase composition of the synthesis products, the diffractogram was processed using the computer software Mash! Crystal Impact ver. 3.3 with FullProf toolbar [20] and the databases SCDD PDF-2, COD (Crystallography Open Database).

The Rietveld method and the Jana2020 program [21] were used to quantify the phase content in the sample. The calculations were based on the X-ray data of the crystallographic open access database (COD) [22] for the compounds: NaCl, KCl, CeF_3, EuF_2, EuF_3. The calculation error did not exceed 2.5%.

2.3. Spectroscopic Methods

The following spectroscopic methods were used: IR transmission spectroscopy, diffuse reflection spectroscopy (DR) and luminescence spectroscopy.

2.3.1. IR Transmittance Spectroscopy

IR spectra were recorded in coordinates $T = f(\tilde{\nu})$, where T, $\tilde{\nu}$ are transmission and wave number, respectively, on a Fourier transformed IR Frontier Perkin-Elmer spectrophotometer (USA) in the range of wave numbers 4000-200 cm^{-1}. CsI-based samples were prepared according to a standard technique.

2.3.2. Diffuse Reflectance Spectroscopy

Diffuse reflectance spectra were measured using a Lambda-9 spectrophotometer (Perkin-Elmer) in the range of 200-2500 nm as a function of:

$$F(R) = f(\lambda) = (1–R)2 / 2R = k / s, \quad (1)$$

where F(R) is the Kubelka-Munk function; R – relative reflection; k, s is absorption and scattering coefficients, respectively.

2.3.3. Luminescence Spectroscopy

Spectra of luminescence and its excitation were recorded on a Fluorolog FL3-22 Jabine Yvon (France) spectrofluorimeter. A Xenon lamp (model 1907) with a power of 450 W served as the source of radiation excitation. A photomultiplier R928P was used as a radiation detector for the visible region of the spectrum. The excitation wavelength range was from 240 to 600 nm, and the luminescence wavelength range was from 290 to 850 nm. The photomultiplier registers the radiation intensity by counting single photons of light and maintains its proportionality in the range of 1,000-2,000,000 counts per second (CPS). Based on this range of sensitivity, the input and output slits of the device were selected. Luminescence measurements were performed in a special cuvette for solid powder materials with a depth of 1.5 mm and a surface area of 70 mm^2. Before recording the luminescence spectrum of the crystalline sample, it was ground into a homogeneous fine powder. The integrated luminescence intensity was determined from the area corresponding to the emission band using the ORIGIN8 program. The radiation wavelength was converted into wave numbers.

To measure the Eu^{3+} luminescence lifetime, the Xenon lamp was switched to pulse mode with the pulse duration of 3 μs. To measure the Eu^{2+} luminescence lifetime, an ultraviolet NanoLED with a $\lambda_{exc.}$ = 330 nm output was used, as well as pulse width 1.4 ns and pulse frequency – 25 kHz.

2. Results and Discussion

3.1. X-ray Diffractogram

The diffractogram obtained for the solidified melt solution NaCl–KCl–EuF_3 (Figure 1) is similar to the diffractogram of NaCl–KCl–CeF_3–EuF_3, which indicates the insignificant content of the dispersed phase (CeF_3, EuF_3) and the significant predominance of the salt matrix.

 doi:10.20944/preprints202410.1383.v1

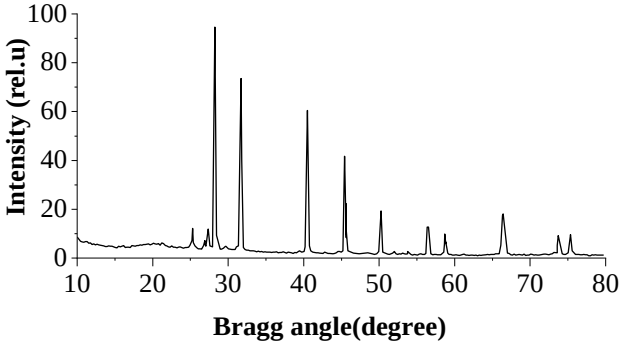

Figure 1. Diffractogram of solidified NaCl–KCl–EuF_3 solution-melt.

The EuF_3 content in the upper part of the solidified melt was 0.3% according to XRD data.

3.2. Results of Spectroscopic Studies

3.2.1. Results of IR Transmission Spectroscopy

The IR transmission spectra (Figure 2, curve 1) of a sample of the CeF_3+EuF_3 system in the region of 250-500 cm^{-1} show two peaks corresponding to the vibrations of the Ce–F and Eu–F bonds (a band in the region of 1100-1200 cm^{-1} appeared, apparently, due to an admixture of Si–O during calcination of the sample in a vessel made of quartz glass). A less pronounced band at ~750 cm^{-1} probably corresponds to the vibrations of Ce–O bonds, which arise due to the pyro-hydrolysis of one of the reaction products, namely, CeF_4.

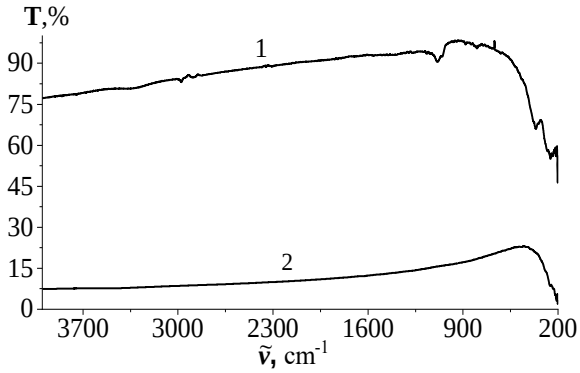

Figure 2. IR transmission spectra of system samples: 1 – CeF_3+EuF_3 after calcination; 2 – NaCl–KCl–CeF_3–EuF_3 (upper part of the solidified salt melt).

The level of transmittance of the sample is very high – 75-95%, which indicates its high crystallinity.

In the samples containing a chloride melt in their base, i.e. a solidified solution – melt, the bands corresponding to the vibrations of the bonds of the base – NaCl and KCl in the region of $\tilde{\nu}$ near 210-220 cm^{-1} are the most prominent on the IR transmission spectrum, on the other hand the bands corresponding to the soluble substance are much weaker (Figure 2, curve 2).

Due to the significantly lower heat treatment temperature of the salt melt samples, they also lack the already mentioned vibration band of Si–O bonds. The transparency of samples of the NaCl–KCl–CeF_3–EuF_3 system is significantly lower, which is most likely an indication of the ultra-micro-disperse composition of the solidified melts.

3.2.2. Results of Diffuse Reflectance Spectroscopy

 doi:10.20944/preprints202410.1383.v1

The analysis of the diffuse reflection spectra of the samples of the studied system confirms in general the predicted nature of the interaction. Thus, on the spectral dependence F(R) = f(λ) of the CeF_3+EuF_3 sample in the near-IR range of the spectrum (1900-2300 nm), weak remnants of the band corresponding to 4f-4f electronic transitions in the Eu^{3+} ion were detected (Figure 3c, curve 1). The intensity of this residual band is 20-30 times lower compared to that of the initial compound EuF_3, which indicates a significant decrease in the content or even the disappearance of the phase of the specified composition. Instead, an absorption band consisting of two broad bands of high intensity, which is characteristic of 4f-5d electronic transitions in Eu^{2+} ions, appears in the UV range of the spectrum (Figure 3a, curve 1), with a partial overlap of $Ce^{3+} \rightarrow Ce^{4+}$ charge transfer bands. So, most likely, the $EuCeF_6$ compound of possible hexagonal local symmetry is formed in the system. More precisely, it can be its component, EuF_2 that passes into the NaCl–KCl melt when they interact with each other.

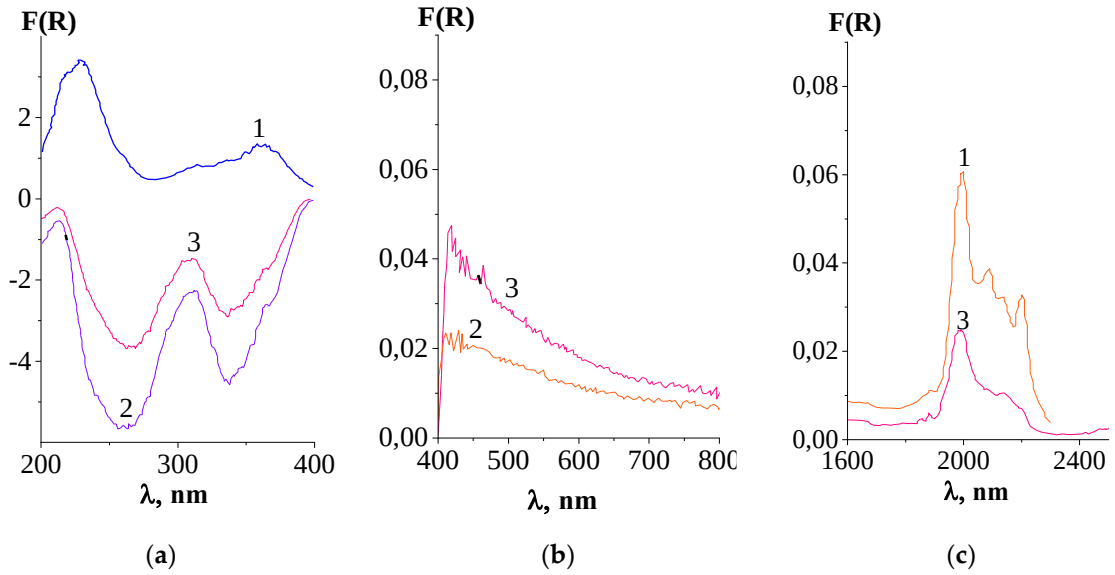

Figure 3. Diffuse reflectance spectra (a – UV, b – visible, c – near-IR ranges) of system samples: 1 – CeF_3+EuF_3 after calcination; 2 – NaCl–KCl–CeF_3–EuF_3 (the upper part of the solidified salt melt); 3 – NaCl–KCl–CeF_3–EuF_3 (insoluble sediment).

The diffuse reflectance spectrum of the NaCl–KCl–CeF_3–EuF_3 liquid in the UV range (Figure 3a, curves 2, 3) is a band with negative absorption consisting of two peaks, which is the manifestation of luminescence in the near visible range of the spectrum. At the same time, the intensity (depth) of the peaks of the homogeneous solidified salt melt (the upper part of the solidified salt melt) is more than 2 times higher than that of the insoluble sediment. It should be noted that for the upper part of the solidified salt melt in the near-IR range of the spectrum, there are no peaks and absorption bands. This is the evidence in favour of the presence of only Eu(II) compounds and the absence of Eu(III) ones.

The diffuse reflectance spectrum of the insoluble sediment in the near-IR range of the spectrum contains a broad, weakly separated absorption band of 4f-4f electronic transitions in Eu^{3+} ions of very weak intensity (almost 2.5 times weaker than that of the CeF_3+EuF_3 sample) (Figure 3c, curve 3). As for Ce(III) and Ce(IV) compounds, it is quite difficult to establish their presence or absence from the diffuse reflectance spectra.

3.2.3. Results of Luminescence Spectroscopy

The method of photoluminescence spectroscopy was used for the identification and detection of Eu^{3+}, Eu^{2+} and Ce^{3+} ions (as well as for a qualitative comparative assessment of their content according to the «more-less» principle) in connection with the presence of characteristic emission bands of these ions due to 4f-4f (Eu^{3+}) and 4f-5d (Eu^{2+} and Ce^{3+}) electronic transitions [23–25].

 doi:10.20944/preprints202410.1383.v1

By changes in the spectra (presence or shift of radiation bands, their splitting, intensity), it is possible to assess the processes that occur in the systems under study, namely, in CeF_3+EuF_3 samples with different ratios of components synthesized in a melt solution of an equimolar mixture of NaCl–KCl.

The emission and luminescence spectra of the studied systems were compared with the spectra of a number of initial samples. Figure 4 shows the excitation and luminescence spectra of the initial CeF_3 and EuF_3 fluorides.

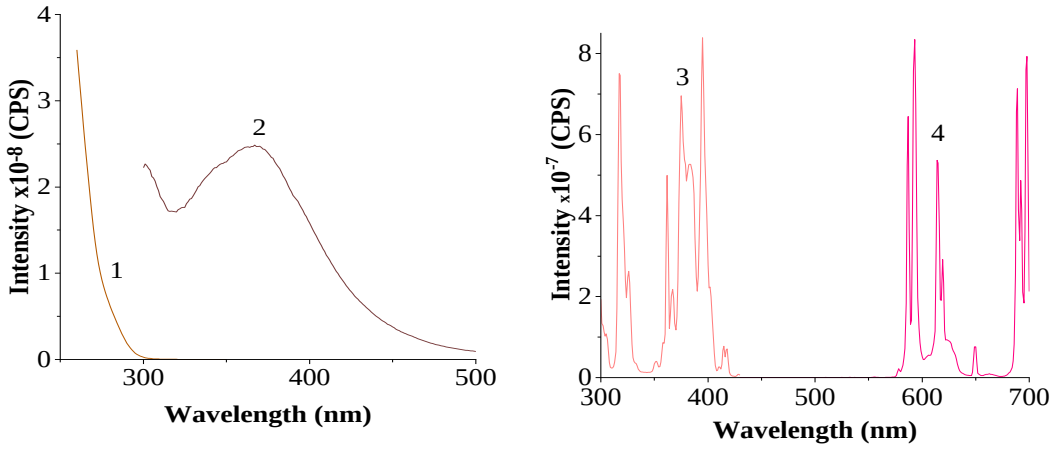

Figure 4. Excitation and luminescence spectra of the initial CeF_3 and EuF_3 samples: 1 – excitation spectrum of Ce^{3+}, recorded at $\lambda_{em.}$ = 367 nm; 2 – luminescence spectrum of Ce^{3+} at $\lambda_{exc.}$ = 265 nm, slits 2.0-2.0 nm; 3 – excitation spectrum of Eu^{3+}, recorded at $\lambda_{em.}$ = 593 nm; 4 – luminescence spectrum of Eu^{3+}, recorded at $\lambda_{exc.}$ = 395 nm, slits 1.5-1.5 nm.

Some characteristic bands with a maximum at 395 nm in the most intense of them can be observed in the excitation spectrum of EuF_3, which in a certain approximation, can be considered as an analogue of the absorption spectrum (diffuse reflection) recorded at $\lambda_{em.}$ = 593 nm. A similar maximum is recorded in the diffuse reflection spectrum of EuF_3 ($\lambda_{max.}$ = 393.7 nm) [26]. In the luminescence spectrum, the peaks characteristic of Eu^{3+} and related to $^5D_0 \rightarrow {}^7F_1$ ($\lambda_{max.}$ 587, 593 nm), $^5D_0 \rightarrow {}^7F_2$ ($\lambda_{max.}$ 615, 620nm), $^5D_0 \rightarrow {}^7F_3$ ($\lambda_{max.}$ 649 nm) and $^5D_0 \rightarrow {}^7F_4$ transitions are recorded ($\lambda_{max.}$ 689, 692, 698 nm) with characteristic splitting and relative peak values.

The CeF_3 luminescence spectrum contains one broad diffuse band with a blurred maximum at 365-372 nm, whose position (according to previous studies) does not depend on the excitation wavelength.

The luminescence spectrum of the mechanical mixture CeF_3:EuF_3 (1:1), as expected, contains emission bands of Ce^{3+} and Eu^{3+}, however, a minimum in the region of 398 nm is observed on the spectral curve caused by 4f-5d-electron transitions in the Ce^{3+} ion, and the main maximum of the band is hypsochromically shifted ($\lambda_{max.}$ = 336 nm) compared to the spectrum of the initial CeF_3. An almost identical picture is observed in the spectra (not shown here) of a mechanical mixture with a ratio of CeF_3:EuF_3 components (1:2), where a minimum on the emission curve of Ce^{3+} ($\lambda_{min.}$ = 398 nm) and a hypsochromic shift of the main maximum ($\lambda_{max.}$ = 332 nm) were also detected. The Eu^{2+} peak is not recorded. The position of the characteristic peaks in the excitation spectrum of the Eu^{3+} sample (317, 374, 394 nm) correlates well with the position of the bands in its diffuse reflectance (DR) spectrum (318, 375, 385 nm).

The spectra of NaCl–KCl–CeF_3 (not shown) and NaCl–KCl–EuF_3 systems with fluoride: melt ratio (1:9) were recorded (Figure 5). In the excitation spectrum of the sample EuF_3 ($\lambda_{em.}$ = 435 nm), a broad intense band with three maxima is recorded, which, as will be shown below, is characteristic of all samples containing Eu^{2+}.

 doi:10.20944/preprints202410.1383.v1

The most intense peak for the analysed system is observed at $\lambda_{exc.}$ = 352 nm. It is worth noting that this band coincides with the minimum in the area of negative values of F(R) on the diffuse reflectance spectrum [27]. The luminescence spectra of the upper and lower parts of the sample indicate the appearance of Eu^{2+} ions in the NaCl–KCl–EuF_3 system, as evidenced by the presence of an intense band with a maximum at 434 nm.

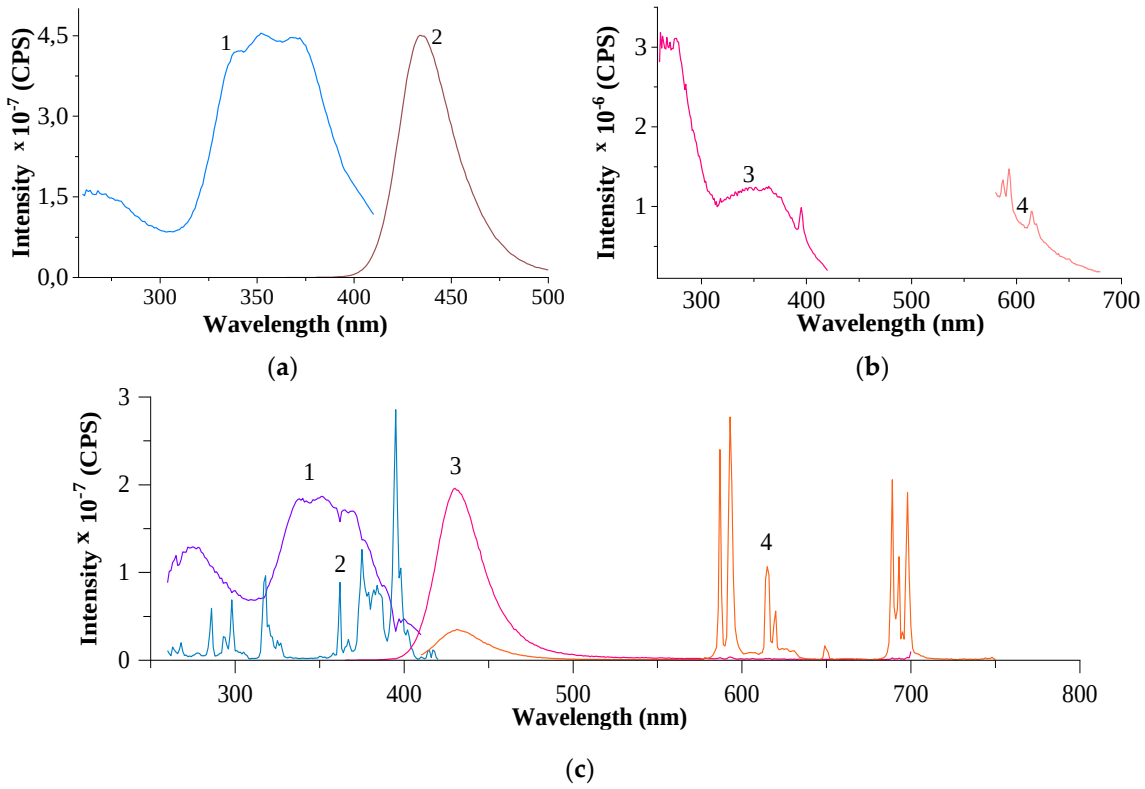

Figure 5. Excitation and luminescence spectra of the upper (a) and lower (b) parts of the EuF_3 melt in NaCl–KCl (1:9): a: 1 – excitation spectrum of Eu^{2+} at $\lambda_{em.}$ = 435 nm, 2 – luminescence spectrum of Eu^{2+} at $\lambda_{exc.}$ = 352 nm, slits 0.6-0.6 nm; 3 – excitation spectrum of Eu^{3+} at $\lambda_{em.}$ = 615 nm, 4 – luminescence spectrum of Eu^{3+} at $\lambda_{exc.}$ = 394 nm, slits 2.0-2.0 nm; b: 1 – excitation spectrum of Eu^{2+} at $\lambda_{em.}$ = 435 nm, 2 – excitation spectrum of Eu^{3+} at $\lambda_{em.}$ = 593 nm; 3 – luminescence spectrum of Eu^{2+} at $\lambda_{exc.}$ = 352 nm, 4 – luminescence spectrum of Eu^{3+} at $\lambda_{exc.}$ = 395 nm, slits 0.6-0.6 nm.

The presence of a significantly smaller amount of Eu^{3+} ions in the upper part compared to the bottom part (insoluble sediment) confirms the proposed mechanism of interaction of EuF_3 with the melt. It consists in the fact that when EuF_3 is dissolved in the NaCl–KCl melt, a redox reaction occurs according to the scheme:

$$EuF_3 + 3NaCl \xrightarrow{T,\,He} EuCl_2 + \frac{1}{2}\,Cl_2\uparrow + 3NaF, \quad (2)$$

and then [28]:

$$2KCl + EuCl_2 \xrightarrow{T,\,He} K_2[EuCl_4]. \quad (3)$$

The luminescence spectrum of the upper part of the NaCl–KCl–CeF_3 sample is similar to the spectrum of the initial CeF_3: the band of the Ce^{3+} ion ($\lambda_{max.}$ = 368 nm) is observed, which is more intense compared to the band of the initial fluoride (2.03×108 and 1.4×108 CPS, respectively), which may indicate reduction in dissolution and, accordingly an effect of concentration quenching. It was interesting to find out how the addition of Ce^{3+} ions to the salt melt affects the emission intensity of Eu^{2+} ions.

 doi:10.20944/preprints202410.1383.v1

In order to find the optimal synthesis conditions and composition, its various parameters were varied. Figure 6 shows the excitation and luminescence spectra of the sample obtained by dissolving the mechanical mixture CeF_3:EuF_3 (1:1) in NaCl–KCl at a temperature of 800°C and holding for 4 hours.

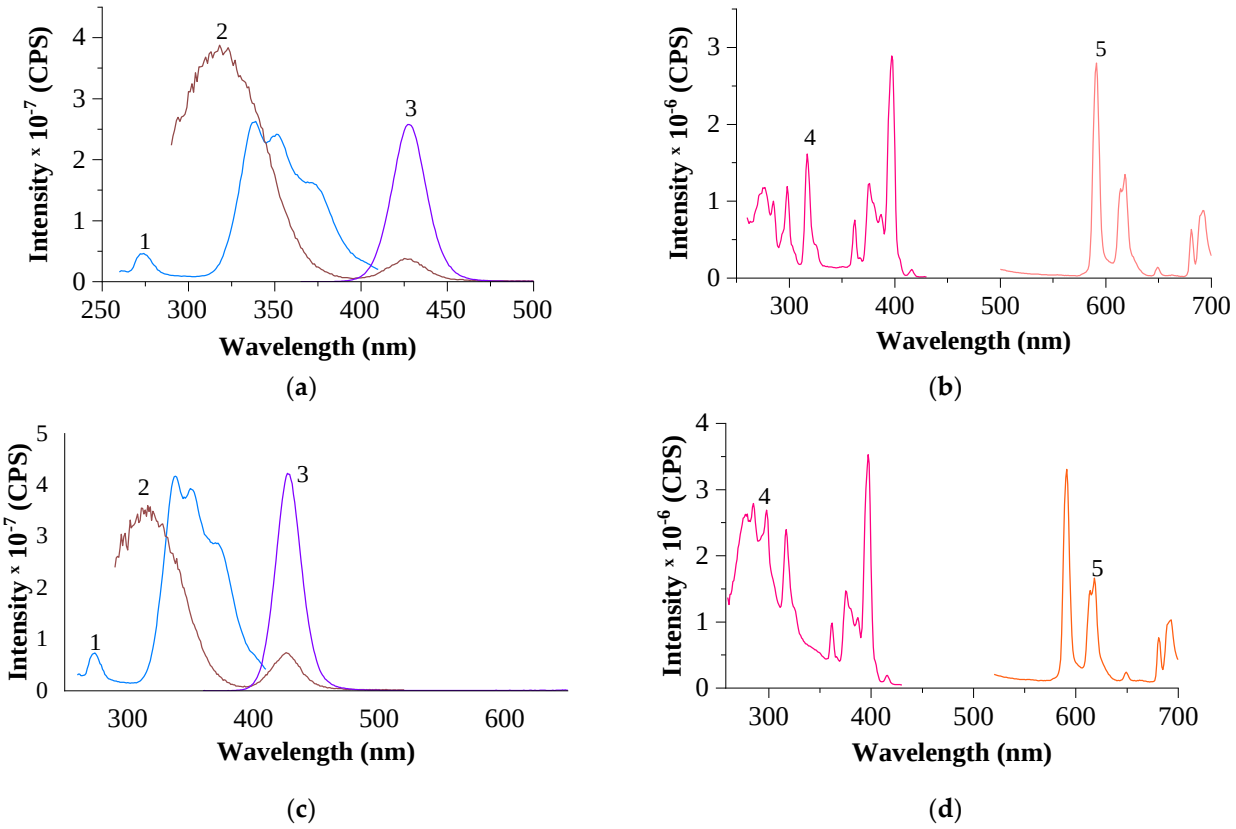

Figure 6. Excitation and luminescence spectra of the upper part of the melt (a) and the bottom part (b) of the melt of a mechanical mixture of CeF_3+EuF_3 (1:1) in NaCl–KCl (1:9): a: 1 – excitation spectrum of Eu^{2+} at $\lambda_{em.}$ = 428 nm, 2 – luminescence spectrum of Ce^{3+} at $\lambda_{exc.}$ = 274 nm, 3 – luminescence spectrum of Eu^{2+} at $\lambda_{exc.}$ = 338 nm, slits 0.6-0.6 nm; 4 – excitation spectrum of Eu^{3+} at $\lambda_{em.}$ = 591 nm; 5 – luminescence spectrum of Eu^{3+} at $\lambda_{exc.}$ = 396 nm, slits 3.0-3.0 nm. b: 1 – excitation spectrum of Eu^{2+} at $\lambda_{em.}$ = 428 nm, 2 – luminescence spectrum of Ce^{3+} at $\lambda_{exc.}$ = 273 nm, 3 – luminescence spectrum of Eu^{2+} $\lambda_{exc.}$ = 340 nm, slits 0.6-0.6 nm; 4 – excitation spectrum of Eu^{3+} at $\lambda_{em.}$

The maximum in the broad diffuse band (Eu^{2+}) is fixed at 340 nm in the excitation spectra recorded at $\lambda_{em.}$ = 428 nm. There is also a maximum at 274 nm, which belongs to the excitation spectrum of Ce^{3+}. The following emission bands are observed in the luminescence spectra: Ce^{3+} – intense, with a hypsochromic shift of the emission maximum at $\lambda_{max.}$ = 318 nm, Eu^{2+} is also intense with $\lambda_{max.}$ = 427 nm and low-intensity Eu^{3+} bands corresponding to $^5D_0 \rightarrow {}^7F_1$ and $^5D_0 \rightarrow {}^7F_4$ electronic transitions with a change in splitting.

The spectra of the bottom and upper parts of the sample are identical in the nature and position of the maxima and differ little in the intensity of the bands. Obviously, the sample of the system solidified salt melt is quite homogeneous.

Figure 7 shows the spectra of the system obtained under similar conditions, but from a mixture of CeF_3 and EuF_3 calcined at 1100°C. The excitation spectra of Eu^{2+} contain three characteristic maxima with the most intense one recorded at 350 nm (upper part of the sample) and 373 nm (bottom part). In the spectrum of the bottom part, an excitation band of Ce3+ ($\lambda_{max.}$ 270 nm) is observed, which is practically absent in the spectrum of the upper part. The excitation spectrum of Eu^{3+} resembles a similar spectrum of the calcined CeF_3+EuF_3 mixture. = 591 nm, 5 – luminescence spectra of Eu^{3+} at $\lambda_{exc.}$ = 397 nm, slits 3.0-3.0 nm.

 doi:10.20944/preprints202410.1383.v1

No Ce^{3+} bands were recorded in the luminescence spectra of both the bottom and upper parts; there are bands characteristic of Eu^{2+} and Eu^{3+}, and the intensity of the emission bands of the latter is significantly higher in the bottom part. It is obvious that under the selected synthesis conditions, oxidation-reduction reactions are shifted towards the formation of Eu^{2+}. If we take into account, the possibility of a reaction during calcination according to the scheme:

$$CeF_3 + EuF_3 \xrightarrow{T,\ He} CeF_4\uparrow + EuF_2, \quad (4)$$

and then,

$$EuF_2 + CeF_4 \xrightarrow{T,\ He} EuCeF_6, \quad (5)$$

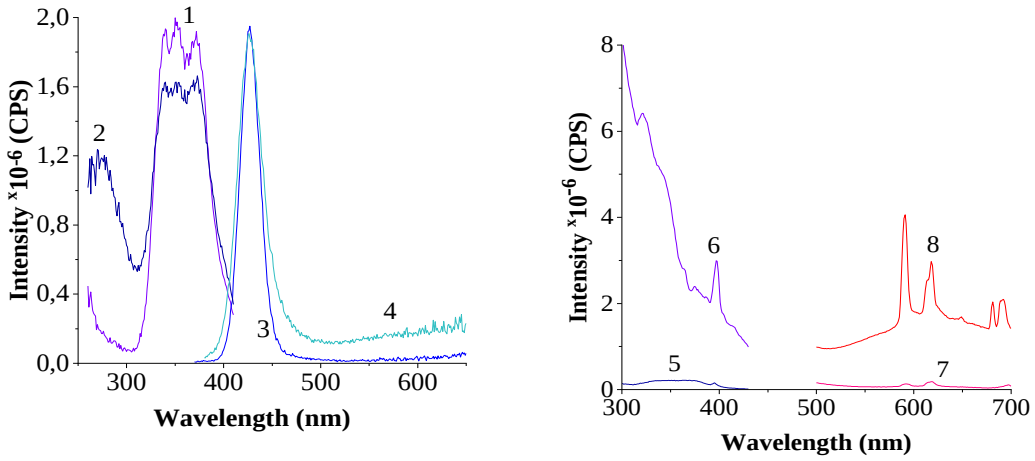

(**a**) (**b**)

Figure 7. Excitation and luminescence spectra of the bottom and upper parts of the sample CeF_3+EuF_3 (1:1) in NaCl–KCl (1:9): a – excitation and luminescence spectra of Eu^{2+}, slits 0.6-0.6 nm; 1 – excitation spectrum at $\lambda_{em.}$ = 428 nm (upper part), 2 – $\lambda_{em.}$ = 426 nm (bottom part); 3 – luminescence spectrum at $\lambda_{exc.}$ = 352 nm (upper part), 4 – $\lambda_{exc.}$ = 352 nm (bottom part); b – excitation and luminescence spectra of Eu^{3+}, slits 3.0-3.0 nm; 5 – excitation spectrum at $\lambda_{em.}$ = 613 nm (upper part), 6 – $\lambda_{em.}$ = 618 nm (bottom part); 7 – luminescence spectrum at $\lambda_{exc.}$ = 395 nm (upper part), 8 – $\lambda_{exc.}$ = 397 nm (bottom part).

it becomes clear where CeF_3 could go, and therefore Ce^{3+} ions from the melt solution.

In order to study the composition, the initial CeF_3+EuF_3 mixture was slightly changed – from the ratio 1:1 to 1:2.

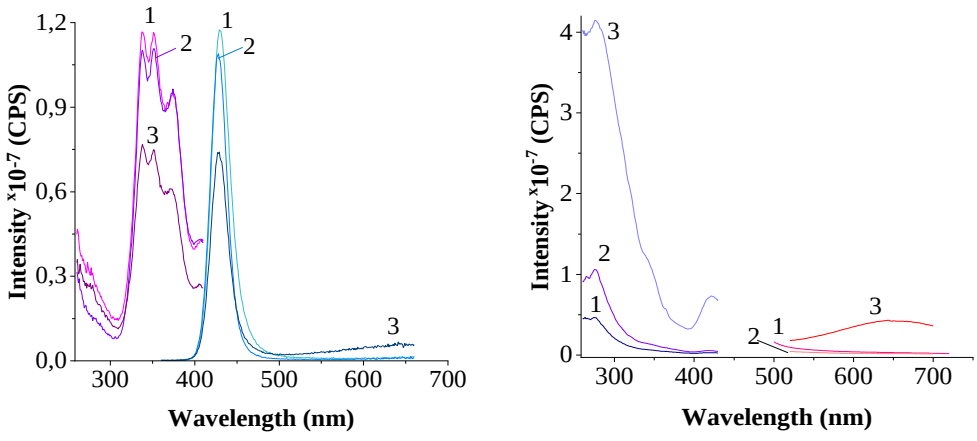

(**a**) (**b**)

 doi:10.20944/preprints202410.1383.v1

Figure 8. Excitation and luminescence spectra of the upper (1), middle (2) and bottom (3) parts of the sample CeF_3+EuF_3 (1:2) in NaCl–KCl (1:9): a – excitation and luminescence spectra of Eu^{2+}: $\lambda_{em.}$ = 429 nm, $\lambda_{exc.}$ = 338 nm, slits 0.6-0.6 nm; b – excitation and luminescence spectra of Eu^{3+}: $\lambda_{em.}$ = 591 nm, $\lambda_{exc.}$ = 397 nm, slits 3.0-3.0 nm.

Figure 8 shows the luminescence spectra of the CeF_3:EuF_3 (1:2) system (calcination at 1100°C). The excitation and luminescence spectra of the upper and middle parts of the sample practically coincide; the spectra of the bottom part have a similar character (except for the luminescence spectrum at $\lambda_{exc.}$ = 398 nm in the bottom part). It should be noted that the bands of Eu^{3+} ions are neither recorded in the excitation spectra, nor in the luminescence spectra. Clearly pronounced bands of Eu^{2+}; and the Ce^{3+} ion (assessed by the excitation spectra) may be present only in trace amounts.

According to Figure 9, for a CeF_3-EuF_3 (1:2) sample obtained from a mechanical mixture in a vacuum (2 hours) at 750°C and a charge ratio : solidified salt melt (2:8), typical excitation spectra of Ce^{3+} (except for the bottom part) and Eu^{3+} appear.

There appears one maximum (two in the spectrum of the bottom part) at 338-340 nm in the broad diffuse band of the Eu^{2+} excitation spectrum. Meanwhile, in the emission spectra recorded at λexc. = 273 nm (optimal for Ce^{3+}), both Cerium and Eu^{2+} bands are recorded. The intensity of Eu^{3+} emission bands is highest in the bottom part.

In the excitation spectra of a sample with a ratio of CeF_3:EuF_3 (2:1), obtained from a mechanical mixture in a vacuum (2 hours) at 750°C and a ratio of a mixture of fluorides: salt melt (2:8) (Figure 9), a characteristic band for Ce^{3+} is manifested only in the spectrum of the upper part of the solidified salt melt, and is absent in the spectrum of the bottom part.

In the Eu^{3+} excitation range, the intensity of the characteristic bands is much higher in the bottom part. In the emission spectra recorded at $\lambda_{exc.}$ = 273 nm, the characteristic band of Ce^{3+} is weak and appears only in the spectrum of the upper part, however, in the spectra of both parts there is a band of Eu^{2+}, whose intensity (as in the case of the previous sample) is higher (or, in the case of the bottom part, is practically equal) than that of similar bands recorded at excitation wavelengths inherent in divalent Europium. The intensity of the emission bands in the range of trivalent Europium is very low.

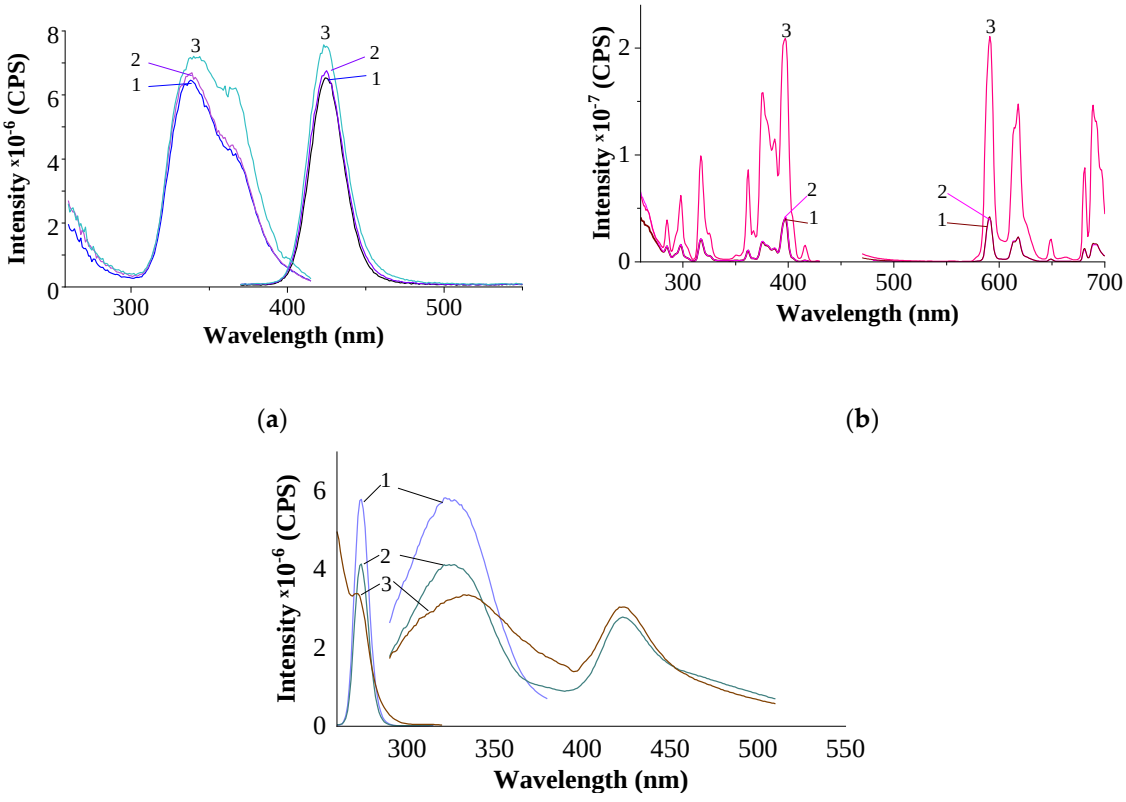

 doi:10.20944/preprints202410.1383.v1

(**c**)

Figure 9. Excitation and luminescence spectra of the upper (1), middle (2) and bottom (3) parts of the sample CeF_3+EuF_3 (1:2) in NaCl–KCl (2:8), 750°C for 2 hours in a vacuum: a – excitation and luminescence spectra of Eu^{2+}: λem. = 425 nm, $\lambda_{exc.}$ = 338 nm, slits 0.6-0.6 nm; b – excitation and luminescence spectra of Eu^{3+}: $\lambda_{em.}$ = 591 nm, $\lambda_{exc.}$ = 397 nm, slits 3.0-3.0 nm; c – excitation and luminescence spectra of Ce^{3+}: $\lambda_{em.}$ = 325 nm, $\lambda_{exc.}$ = 273 nm, slits 3.0-3.0 nm.

The obtained data show that the interaction in the system takes place most fully (the intensity of luminescence of Ce^{3+} and Eu^{3+} ions is minimal, and the intensity of luminescence of Eu^{2+} ions is maximal) at synthesis with a ratio of mechanical mixture calcined at 1100°C: salt melt as 1:9; similarly, the interaction occurs when the ratio of a mechanical mixture of fluorides: salt melt is 2:8 at 750°C in a vacuum. In both cases, the CeF_3:EuF_3 ratio was 1:2. Since the studied objects are of interest as promising materials for ultraviolet radiation detectors, the Eu^{2+} luminescence spectra (the upper part of the solidified salt melt) were recorded first for the samples at different excitation wavelengths in the UV range of the spectrum. The results are presented in Table 1.

It can be seen from Table 1 that when the sample is excited by radiation in almost the entire UVA-UVB range of wavelengths, a very intense luminescence of Eu^{2+} ions is observed with its maximum values at $\lambda_{exc.}$ = 340-350 nm. At the same time, the intensity at the maximum point ($I_{max.}$) and the integrated intensity ($I_{int.}$) reach their highest values in the excitation wavelength range of 330-375 nm. A qualitative correlation is observed between the luminescence excitation spectrum and the spectrum of solar radiation in the ultraviolet range [1].

The position of the radiation maximum ($\bar{\lambda}_{max.}$ = 430 nm) practically does not depend on the excitation wavelength in the investigated wavelength range.

Table 1. This is a table. Tables should be placed in the main text near to the first time they are cited.

no pos.	Wavelength, nm		Intensity	
	$\lambda_{exc.}$	$\lambda_{max.}$	$I_{max.}\times10^{-6}$, CPS	$I_{int.}\times10^{-7}$, rel. u.
1	261	431	4.53	14.30
2	300	432	1.66	6.19
3	310	432	1.55	5.44
4	317	430	2.20	7.85
5	330	429	7.31	22.79
6	340	430	11.7	34.91
7	350	430	11.1	32.74
8	362	430	8.95	26.98
9	375	430	9.04	26.42
10	387	430	5.57	16.20
11	397	430	3.87	10.48

The luminescence lifetimes (τ) of Eu^{2+} and Eu^{3+}, calculated from the decay curves for various samples, are presented in Table 2.

Table 2. Luminescence lifetime of Eu^{2+} and Eu^{3+} ions in the upper part of samples synthesized from a mechanical mixture of fluorides by heat treatment in a NaCl–KCl melt, vacuum, 750°C ($\lambda_{exc.}$ of Eu^{2+} = 338 nm; $\lambda_{exc.}$ of Eu^{3+} = 398 nm).

no pos.	Sample	Eu^{2+}		Eu^{3+}	
		$\lambda_{max.}$, nm	τ, μs	$\lambda_{max.}$, nm	τ, μs
1	CeF_3+EuF_3(1:1) + NaCl–KCl (1:9)	428*	1.07	591	1301

 doi:10.20944/preprints202410.1383.v1

2	CeF_3+EuF_3(1:2) + NaCl–KCl (2:8)	424*	1.00	591	699**
3	CeF_3+EuF_3(2:1) + NaCl–KCl (2:8)	428*	1.02	591	975**

* – diode lamp; ** – average of 2 measurements.

The luminescence lifetime of Eu^{2+} ions, determined in this paper, is about 1 μs; for Eu^{3+} ions, it varies in the range of 700-1300 μs, that is, more than a thousand times higher. This fact is consistent with generally accepted ideas about the mechanisms of excitation and emission of Eu in different valence states.

4. Conclusions

The results of diffuse reflectance spectroscopy and luminescence spectroscopy of the NaCl–KCl–CeF_3–EuF_3 system regarding the reduction of Eu(III) to Eu(II) agree satisfactorily with each other. The obtained data show that the redox interaction of CeF_3 and EuF_3 with the NaCl–KCl melt occurs most completely at a ratio of 1:9 with preliminary calcination of fluoride components at 1100°C, as well as at a mass ratio of 2:8 of the mechanical mixture of fluorides to the salt melt, and the ratio of CeF_3 to EuF_3 1:2. The result is the maximum luminescence intensity of Eu^{2+} ions at an excitation wavelength of 340-350 nm and the minimum intensity of Eu^{3+} and Ce^{3+} ions. The research is promising for the creation of detectors of ultraviolet solar radiation.

5. Patents

The method for the obtaining the material for detectors of the solar ultraviolet radiation is protected by Ukrainian patent no. 152026.

Supplementary Materials: The following supporting information can be downloaded at the website of this paper posted on Preprints.org, Figure S1: title; Table S1: title; Video S1: title.

Author Contributions: Viktor Zinchenko: conceptualization, methodology, data visualization, formal analysis, resources, data curation, funding acquisition, writing-original draft preparation, project administration. Ganna Volchak: conceptualization, data visualization, formal analysis, data curation, visualization, software. Natalia Chivireva: conceptualization, writing-original draft preparation, writing-review and editing, supervision. Pavlo Doga: methodology, investigation, writing-review and editing, software. Yaroslav Bobitski: formal analysis, visualization. Oleh Ieriomin: methodology, investigation, resources. Smola Serhiy: methodology, investigation. Anton Babenko: investigation, resources. Małgorzata Sznajder: project administration, resources, validation. All authors have read and agreed to the published version of the manuscript.

Funding: Please add: This research was funded by the National Academy of Sciences of Ukraine, within grant no. II.1.22(428) / 0122U000854. The article processing charge was financed by the Institute of Physics University of Rzeszow.

Data Availability Statement: The raw/processed data required to reproduce these findings can be obtained from the corresponding author (volchakganna@gmail.com) upon reasonable request..

Acknowledgments: The authors would like to thank Volodymyr Dotsenko, head of Department of Chemistry of Lanthanides, Bogatsky Physico-Chemical Institute of NAS of Ukraine for valuable advices concerning the luminescent spectroscopy measurements

Conflicts of Interest: The authors declare no conflicts of interest.

References

1. Hoerter, J. D.; Ward, C. S.; Bale, K. D.; Gizachew, A. N.; Graham, R.; Reynolds, J.; Ward, M. E.; Choi, C.; Kagabo, J.-L.; Sauer, M.; Kuipers, T.; Hotchkiss, T.; Banner, N.; Chellson, R. A.; Ohaeri, T.; Gant, L.; Vanderhill, L. Effect of UVA Fluence Rate on Indicators of Oxidative Stress in Human Dermal Fibroblasts. *Int. J. Biol. Sci.* **2008**, 63–70. https://doi.org/10.7150/ijbs.4.63.
2. Luff, B. J.; Townsend, P. D. High Sensitivity Thermoluminescence Spectrometer. *Meas. Sci. Technol.* **1993**, *4* (1), 65–71. https://doi.org/10.1088/0957-0233/4/1/011.
3. Zou, Y.; Zhang, Y.; Hu, Y.; Gu, H. Ultraviolet Detectors Based on Wide Bandgap Semiconductor Nanowire: A Review. *Sensors* **2018**, *18* (7), 2072. https://doi.org/10.3390/s18072072.

4. Blasse, G.; Grabmaier, B. C. *Luminescent Materials*; Springer Berlin Heidelberg: Berlin, Heidelberg, 1994. https://doi.org/10.1007/978-3-642-79017-1.
5. Van Krevel, J. W. H.; Hintzen, H. T.; Metselaar, R.; Meijerink, A. Long Wavelength Ce3+ Emission in Y–Si–O–N Materials. *Journal of Alloys and Compounds* **1998**, *268* (1–2), 272–277. https://doi.org/10.1016/S0925-8388(97)00550-1.
6. Xu, S.; Li, P.; Wang, Z.; Li, T.; Bai, Q.; Sun, J.; Yang, Z. Luminescence and Energy Transfer of Eu^{2+}/Tb^{3+}/Eu^{3+} in $LiBaBO_3$ Phosphors with Tunable-Color Emission. *J. Mater. Chem. C* **2015**, *3* (35), 9112–9121. https://doi.org/10.1039/C5TC01577D.
7. Li, T.; Li, P.; Wang, Z.; Xu, S.; Bai, Q.; Yang, Z. Coexistence Phenomenon of Ce^{3+}–Ce^{4+} and Eu^{2+}–Eu^{3+} in Ce/Eu Co-Doped $LiBaB_9O_{15}$ Phosphor: Luminescence and Energy Transfer. *Phys. Chem. Chem. Phys.* **2017**, *19* (5), 4131–4138. https://doi.org/10.1039/C6CP07494D.
8. Aguirre De Carcer, I.; Lifante, G.; Cussó, F.; Jaque, F.; Calderón, T. Europium-Doped Alkali Halides as a Selective Ultraviolet Dosimeter Material in the Actinic Region. *Applied Physics Letters* **1991**, *58* (17), 1825–1826. https://doi.org/10.1063/1.105100.
9. Córdoba, C.; Muñoz, J. A.; Cachorro, V.; Cárcer, I. A. D.; Cussó, F.; Jaque, F. The Detection of Solar Ultraviolet-C Radiation Using KCl:Eu2+ Thermoluminescence Dosemeters. *J. Phys. D: Appl. Phys.* **1997**, *30* (21), 3024–3027. https://doi.org/10.1088/0022-3727/30/21/017.
10. De Cárcer, I. A.; Dántoni, H. L.; Barboza-Flores, M.; Correcher, V.; Jaque, F. KCl: Eu^{2+} as a Solar UV-C Radiation Dosimeter. Optically Stimulated Luminescence and Thermoluminescence Analyses. *Journal of Rare Earths* **2009**, *27* (4), 579–583. https://doi.org/10.1016/S1002-0721(08)60292-6.
11. Cordoba-Jabonero, C.; Aguirre De Carcer, I.; Barboza-Flores, M.; Jaque, F. Solar Ultraviolet-B Detectors Using Eu2+ Doped Alkali Halide Crystals. *Journal of Alloys and Compounds* **2001**, *323–324*, 847–850. https://doi.org/10.1016/S0925-8388(01)01158-6.
12. Bangaru, S.; Muralidharan, G. Luminescence Studies on Gamma Irradiated KCl: Ce^{3+} Crystals. *Physica B: Condensed Matter* **2012**, *407* (12), 2185–2189. https://doi.org/10.1016/j.physb.2012.02.038.
13. Krishnakumar, D. N.; Rajesh, N. P. Growth and Optical Characterization of Europium and Cerium Doped KCl Single Crystals by Czochralski Method for Dosimetric Applications. *Journal of Elec Materi* **2019**, *48* (3), 1629–1633. https://doi.org/10.1007/s11664-018-06863-3.
14. Cheng, S.; Hunneke, R. E.; Tian, M.; Lukosi, E.; Zhuravleva, M.; Melcher, C. L.; Wu, Y. Self-Assembled $^{nat}LiCl$–$CeCl_3$ Directionally Solidified Eutectics for Thermal Neutron Detection. *CrystEngComm* **2020**, *22* (19), 3269–3273. https://doi.org/10.1039/C9CE01884K.
15. Kuznetsov, S. A.; Gaune-Escard, M. Electronic Conductivity of NaCl-KCl Equimolar Melt Containing Eu(III) and Eu(II) Complexes by Electrochemical Impedance Spectroscopy. *Zeitschrift für Naturforschung A* **2006**, *61* (9), 486–490. https://doi.org/10.1515/zna-2006-0906.
16. Fujii, T.; Nagai, T.; Sato, N.; Shirai, O.; Yamana, H. Electronic Absorption Spectra of Lanthanides in a Molten Chloride. *Journal of Alloys and Compounds* **2005**, *393* (1–2), L1–L5. https://doi.org/10.1016/j.jallcom.2004.10.013.
17. Zinchenko, V. F.; Volchak, G. V.; Ieriomin, O. G.; Stoyanova, I. V.; Chivirova, N. O.; Kuleshov, S. V; Doga, P. G.; Spectral Properties of Ultrafine Systems LaF_3 and EuF_3 in a Frozen Melt NaCl-KCl. *Surface.* **2019**, *11(26)*, 394–402. https://doi.org/10.15407/Surface.2019.11.394.
18. Zinchenko, V.; Ieriomin, O.; Volchak, G.; Stoyanova, I. Spectroscopic Study of Stiffened Saline Melts of NaCl–KCl–LnF3 (Ln = La÷Lu) Systems. *Visnyk Lviv Univ. Ser. Chem.* **2020**, *61* (2), 394. https://doi.org/10.30970/vch.6102.394.
19. Zinchenko, V.; Ieriomin, O.; Antonovich, V.; Chivireva, N.; Stoianova, I.; Volchak, G.; Doga, P. SPECTROSCOPIC PROPERTIES OF SOLIDIFIED MELTS OF THE EuF_3-CeF_3-NaCl-KCl SYSTEM. *Ukr. Chem. Journ.* **2020**, *86* (10), 120–128. https://doi.org/10.33609/2708-129X.86.10.2020.120-128.
20. Putz, H. Match! - Phase Analysis Using Powder Diffraction-Version 3. http://www.crystalimpact.com/download/match3/Manual.pdf (accessed 2024-10-09).
21. Petříček, V.; Palatinus, L.; Plášil, J.; Dušek, M. Jana2020 – a New Version of the Crystallographic Computing System Jana. *Zeitschrift für Kristallographie - Crystalline Materials* **2023**, *238* (7–8), 271–282. https://doi.org/10.1515/zkri-2023-0005.
22. Vaitkus, A.; Merkys, A.; Sander, T.; Quirós, M.; Thiessen, P. A.; Bolton, E. E.; Gražulis, S. A Workflow for Deriving Chemical Entities from Crystallographic Data and Its Application to the Crystallography Open Database. *J Cheminform* 2023, 15 (1), 123. https://doi.org/10.1186/s13321-023-00780-2.
23. Dorenbos, P. Ce^{3+} 5d-Centroid Shift and Vacuum Referred 4f-Electron Binding Energies of All Lanthanide Impurities in 150 Different Compounds. *Journal of Luminescence* 2013, 135, 93–104. https://doi.org/10.1016/j.jlumin.2012.09.034.
24. Dorenbos, P. Energy of the First 4f7→4f65d Transition of Eu^{2+} in Inorganic Compounds. *Journal of Luminescence* **2003**, *104* (4), 239–260. https://doi.org/10.1016/S0022-2313(03)00078-4.

25. Lizzo, S.; Velders, A. H.; Meijerink, A.; Dirksen, G. J.; Blasse, G. The Luminescence of Eu2+ in Magnesium Fluoride Crystals. *Journal of Luminescence* **1995**, *65* (6), 303–311. https://doi.org/10.1016/0022-2313(95)00080-1.
26. Antonovich, V. P.; Stoyanova, I. V.; Chivireva, N. A.; Timukhin, E. V.; Zinchenko, V. F.; Efryushina, N. P. Identification and Quantitative Determination of Some Inorganic Lanthanide Compounds by Diffuse Reflectance Spectroscopy. *J Anal Chem* **2007**, *62* (3), 238–244. https://doi.org/10.1134/S1061934807030070.
27. Zinchenko, V. F.; Ieriomin, O. G.; Stoyanova, I. V.; Volchak, G. V.; Babenko, A. V. DIFFUSE REFLECTION SPECTRA OF FROZEN SALT MELTS OF THE CeF_3-EuF_3-NaCl-KCl SYSTEMS. *Odesa National University Herald. Chemistry* **2022**, *27* (2(82)), 20–34. https://doi.org/10.18524/2304-0947.2022.2(82).264881.
28. M. Gaune-Escard, L. Rycerz, E. Ingier-Stocka, S. Gadžurić, Systematics in the formation of lanthanide halide compounds, Proc. Ninth International Conference on Molten Slags, Fluxes and Salts (MOLTEN12), (2012), May 27th-30th, Beijing, China. P. 198. https://www.pyrometallurgy.co.za/MoltenSlags2012/W189.pdf